

# Inversion of the temperature dependence of crystallization rates due to onset of chain folding

G. Ungar and A. Keller

H. H. Wills Physics Laboratory, University of Bristol, Tyndall Avenue, Bristol BS8 1TL, UK

(Received 9 December 1986; revised 9 March 1987; accepted 16 March 1987)

Crystallization rate experiments performed on the uniform alkanes  $C_{246}H_{494}$  and  $C_{198}H_{398}$ , by both differential scanning calorimetry and *in situ* X-ray diffraction (using a synchrotron source), have revealed that these rates, including both primary nucleation and growth, pass through a minimum with increasing supercooling. The first (expected) increase and subsequent (unsuspected) decrease correspond to extended-chain (E) crystallization, the renewed increase beyond the minimum corresponding to chain-folded crystallization with the fold period  $l$  being smaller than  $L$  but larger than  $L/2$ , where  $L$  is the extended chain length. The anomalously retarded crystallization with increasing supercooling, new even qualitatively, appears to arise through competition between extended- and folded-chain deposition. The attachment of folded chains evidently involves a much lower free energy barrier than does the attachment of extended chains. Even if the former process cannot lead to growth of stable chain-folded crystals above their melting temperature, it seriously hampers the only productive process, chain-extended crystallization. The observed effects, which have come to light owing to the availability of ultra-long and uniform n-alkanes, help to provide new insight into the primary stages of chain-folded crystallization, with many potential consequences, some of which are discussed.

(Keywords: crystallization rate minimum; ultra-long alkanes; synchrotron X-ray diffraction; polymer crystallization; chain folding)

## INTRODUCTION

The present work is a further stage in the study of the crystallization behaviour of ultra-long paraffins (up to  $C_{398}H_{798}$ ) of very high purity, such as have become available through the organic chemical synthesis carried out by Whiting and coworkers<sup>1,2</sup>. As described by us earlier<sup>3</sup>, these paraffins provide a unique opportunity to bridge the gap between the extended-chain crystallization of conventional short n-alkanes and the chain-folded crystallization of polyethylene. In the first instance the work was undertaken to elucidate controversial issues relating to chain folding in high polymers. Some success in this direction has already been achieved and more is ahead. However, at the same time new effects have been uncovered, as will be apparent from the present work.

In the first stage of the work, reported in summary in ref. 3, basic chain fold lengths in the crystals were assessed by both low frequency Raman (LAM) and small angle X-ray scattering methods (SAXS). It was found both for melt and solution crystallization that the chains begin to fold at around a chain length corresponding to  $C_{150}H_{302}$  and possibly somewhat below. Further, it was found that the fold length ( $l$ ) was a decreasing function of crystallization temperature ( $T_c$ ) for the same compound. The  $l$  values themselves, as determined after crystallization was complete and at room temperature were found to be integer fractions ( $1/1$ ,  $1/2$ ,  $1/3$ , etc.) of the chain length. It thus follows that the chain ends are at the crystal layer surface. Further, knowing the exact chain length, it could be inferred that the folds are adjacently entrant and essentially sharp.

The above quantized nature of  $l$  was also confirmed in recent morphological studies on solution-grown crystals, with  $l$  values measured by electron microscope. Amongst other results it was found that sectorization, and hence preferential fold plane direction, could be established even for a crystal consisting of merely once-folded chains.

In another stage of the work, crystallization within the melt was followed *in situ* by SAXS using a synchrotron X-ray source regarding  $l$  values in the case of  $C_{246}H_{494}$ <sup>5</sup>. In the temperature range between the melting points of the once- and twice-folded forms, rather unexpectedly, the primary  $l$  value arising was observed to be intermediate between those corresponding to the extended (E) and accurately once-folded – two full stems (F2) – values. This primary form was termed accordingly the non-integer form (NIF). The initial NIF  $l$  values were somewhat dependent on  $T_c$ . The NIF form was found to be transient, as it still transformed during or immediately after crystallization, either to E by isothermal thickening or to F2 by isothermal thinning, according to  $T_c$ . The same happened during cooling at practicable rates, accounting for the integer fraction values usually observed at room temperature (the subject of our first work)<sup>3</sup>. It was inferred that for the primary NIF crystals the fold surface must be highly disordered, regularization setting in only on refolding to the F2 structure. The implications of all these findings will be discussed in relation to polymer crystallization in ref. 6.

The present work is a continuation of the above *in situ* studies on melt crystallization with the aim of following crystallization rates. Information on rates has become

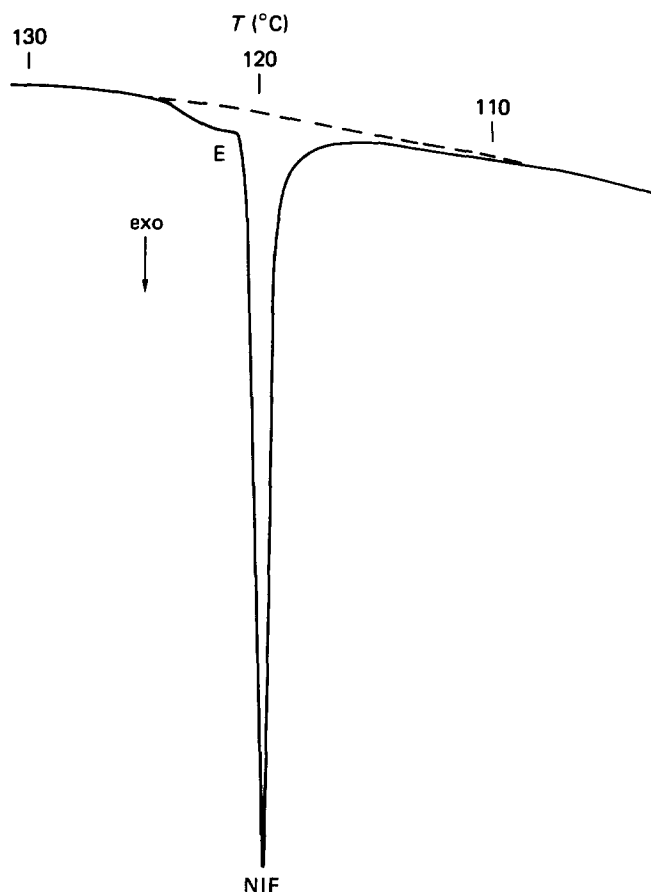


**Figure 1** D.s.c. cooling scan of paraffin  $C_{246}$ , cooling rate  $1^{\circ}\text{C min}^{-1}$ . Crystallization peaks of the extended-chain (E) and folded-chain (NIF) form are marked

available previously<sup>5</sup> through differential scanning calorimetry (d.s.c.) measurements which had been conducted to monitor the course of crystallization as a preliminary to synchrotron X-ray experiments. As briefly mentioned in ref. 5, the d.s.c. traces displayed notable anomalies regarding crystallization rates when going from the E to the NIF state on lowering  $T_c$ . This issue is examined specifically, in the work here described, through combined d.s.c. and synchrotron-based SAXS measurements.

## EXPERIMENTAL

### Materials

n-Alkanes  $C_{246}H_{494}$  and  $C_{198}H_{398}$ , synthesized by Bidd and Whiting<sup>2</sup>, were used for studying crystallization from the melt.

### Calorimetry

A Perkin-Elmer DSC-2 was used for the bulk of the experiments, only the thermogram in Figure 1 being recorded with a DSC-1B instrument.

Crystallization experiments were performed either isothermally or at a constant cooling rate. Temperature was calibrated by determining the melting point of indium at different heating rates and linearly extrapolating the readout error to zero heating rate (for isothermal experiments) or to negative heating rates (for cooling experiments).

### Synchrotron small-angle X-ray scattering (SAXS)

Real-time SAXS experiments on crystallization of long paraffins were carried out on the Daresbury Synchrotron Radiation Source. The procedure has been described previously in some detail<sup>5</sup>. The specimen was held in a 1 mm Lindemann glass capillary thermostatted to  $\pm 0.1^{\circ}\text{C}$  in a modified Mettler hot stage. Absolute temperature was cross-calibrated with d.s.c.

## RESULTS

### Initial observations on $C_{246}$

The unusual shape of the crystallization exotherm produced by cooling molten  $C_{246}H_{494}$  paraffin at  $1^{\circ}\text{C min}^{-1}$  (Figure 1) was noted in the course of our previous study<sup>5</sup> on chain-folded crystallization of this alkane. Noticeable heat evolution starts at  $126^{\circ}\text{C}$ , its rate increasing with increasing supercooling  $\Delta T$ . However, as  $\Delta T$  is increased further a levelling off of the heat evolved, and hence of the gross crystallization rate, follows even at a stage when only a small fraction of material has crystallized. At  $121^{\circ}\text{C}$  crystallization speeds up again, reaching very high rates, and the bulk of the material crystallizes around this temperature.

A parallel SAXS experiment (Figure 2) reveals that the first exotherm in Figure 1 arises from the formation of extended-chain crystals (E form), while the dominant second exotherm is due to once-folded chain crystallization into 'non-integer form' (NIF)<sup>5</sup> (see Introduction).

The shape of the crystallization thermogram in Figure 1 thus suggests that after the initial acceleration, the extended-chain crystallization rate slows down with increasing supercooling as the crystallization temperature corresponding to a transition ( $T^*$ ) between extended and folded-chain crystallization is approached<sup>†</sup>. In view of the uniqueness and potential significance of this finding, further experiments were carried out more systematically, as described below.

### Isothermal crystallization

Isothermal crystallization of  $C_{246}H_{494}$  takes place in a time interval (several minutes to 30 min) convenient for d.s.c. study over almost the entire range of supercoolings that give rise to extended-chain crystals. A series of isothermal crystallization curves were thus recorded for this material. In all cases the paraffin was cooled from the same melt temperature of  $142^{\circ}\text{C}$  to the preset temperature  $T_c$ , employing an identical cooling pattern:  $20^{\circ}\text{C min}^{-1}$  to  $T_c + 2^{\circ}\text{C}$ , followed by  $10^{\circ}\text{C min}^{-1}$  to  $T_c + 1^{\circ}\text{C}$ ,  $5^{\circ}\text{C min}^{-1}$  to  $T_c + 0.5^{\circ}\text{C}$ , and  $2.5^{\circ}\text{C min}^{-1}$  to  $T_c$ . Representative isothermal d.s.c. crystallization curves are shown in Figure 3. The curves indeed confirm the observation of the preliminary experiment and clearly reveal that the overall crystallization rate slows down with increasing supercooling as  $T^*$  is approached. As seen, the extent of this slowdown is remarkable.

For reference, it should be noted that the melting point of well annealed extended-chain  $C_{246}H_{494}$  crystals is  $128.6^{\circ}\text{C}$ . Melting points of the once-folded forms, F2 and NIF, could not be determined with the same accuracy, as discussed previously<sup>5</sup>. This arises for two reasons: first,

<sup>†</sup> Note that there are small differences between the values of  $T^*$  according to whether it refers to crystal growth or primary nucleation, the former being lower in the present case (see later).

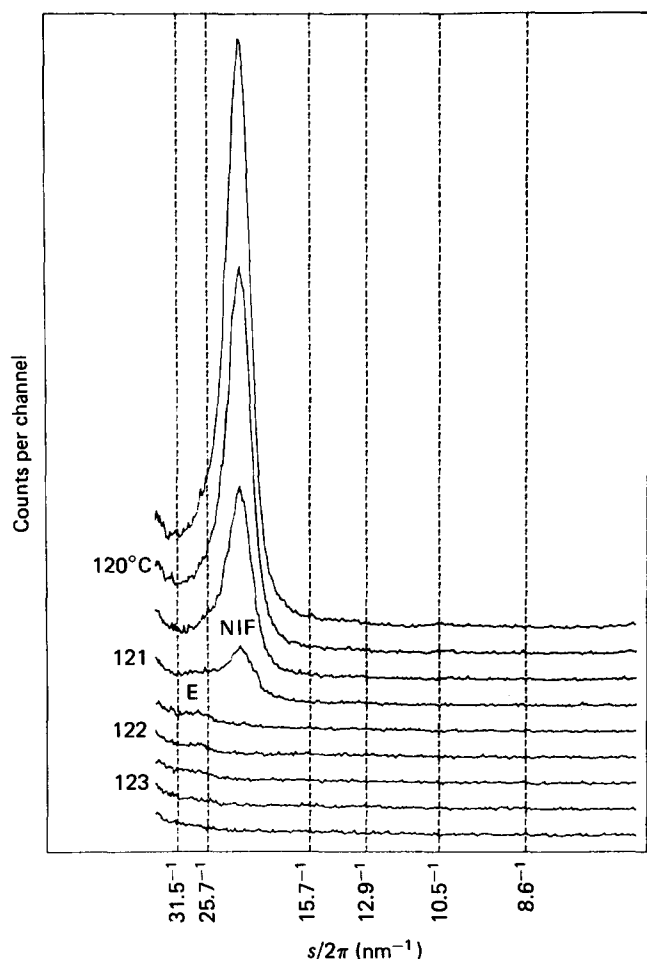


**Figure 2** Synchrotron SAXS curves taken at 30 s intervals during cooling of paraffin  $C_{246}$  at  $1^\circ\text{C min}^{-1}$  (cf. Figure 1). The curves show first the development of the weak first-order diffraction maximum of the tilted extended-chain form (E), followed by that of an intense NIF peak (chains presumed perpendicular<sup>5</sup>). Abscissae are marked corresponding to calculated spacings for perpendicular layers of periodicity  $L$  (extended length, 31.5 nm),  $L/2$  (15.7 nm) and  $L/3$  (10.5 nm), as well as those tilted by  $35^\circ$  (25.7 nm, 12.9 nm and 8.6 nm, respectively)

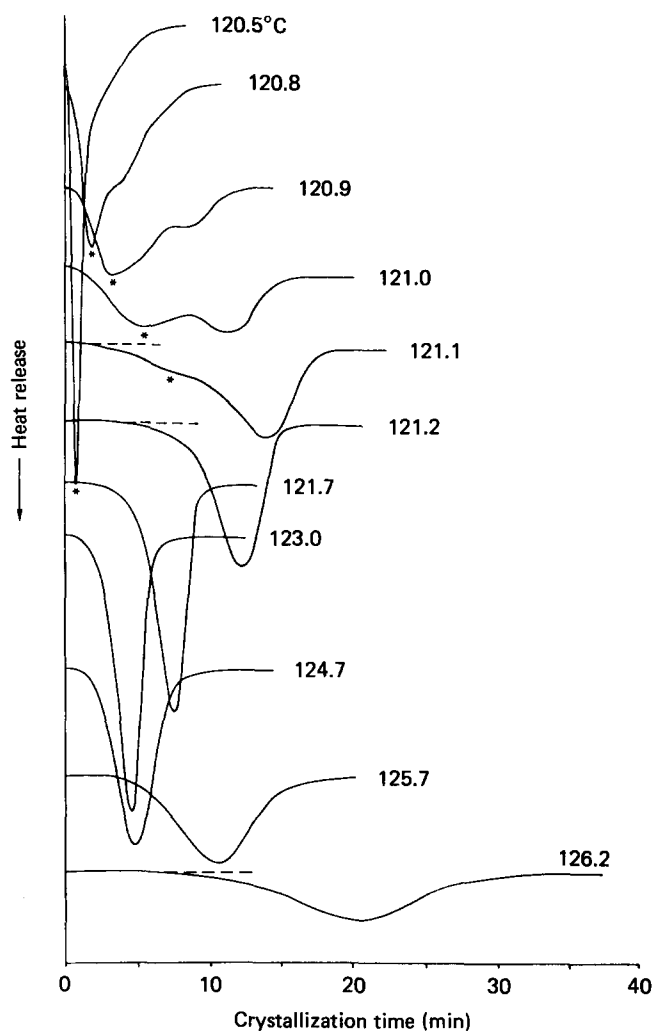


**Figure 3** Isothermal d.s.c. melt-crystallization exotherms of  $C_{246}$ . Peaks marked with an asterisk are due to crystallization with folded chains (NIF) and the unmarked ones to crystallization with extended chains

melting is immediately followed by recrystallization of the E form during heating, and secondly, reversible thickening of NIF ('surface melting') takes place very close to the melting point, giving a broadened melting range<sup>6</sup>. It has been ascertained so far that the  $T_m$ s of both F2 and NIF forms fall within the temperature interval  $(122.5 \pm 1.5)^\circ\text{C}$ .

Two empirical parameters characterizing the isothermal crystallization of  $C_{246}$  paraffin are plotted in Figures 4 and 5 as a function of  $T_c$ . The first parameter is  $1/t_{10}$ , where  $t_{10}$  is the time elapsed between establishing  $T_c$  and reaching 10% crystallization. As the crystallization is controlled by primary nucleation (see later), Figure 4 is expected to represent fairly accurately the temperature variation of the primary nucleation rate. The second parameter is the maximum height of the d.s.c. exotherm, which is proportional to the maximum rate of overall crystallization. With increasing supercooling both parameters first increase and pass through a maximum, which is followed by a deep minimum around  $T^*$ , and finally by a steep increase below  $T^*$  as chain-folded crystallization sets in.

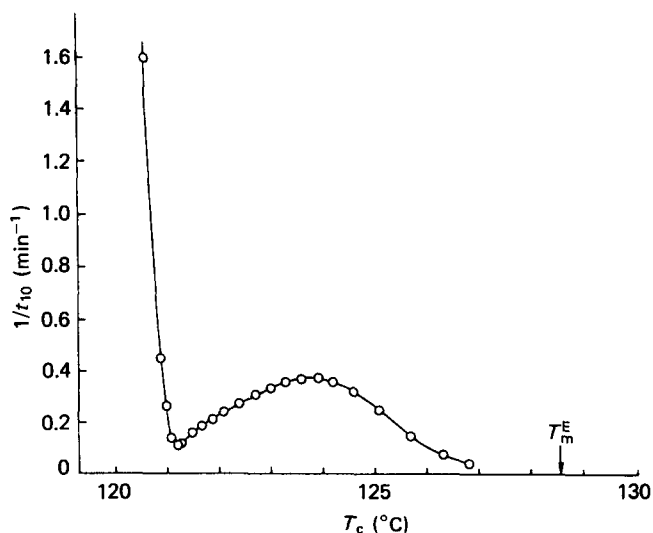


**Figure 4** Reciprocal time  $1/t_{10}$  elapsed between establishing the temperature  $T_c$  and the evolution of 10% of the heat of crystallization, as a function of  $T_c$ ; isothermal crystallization of  $C_{246}$  from the melt. Variation in  $1/t_{10}$  is expected to reflect fairly accurately the variation in primary nucleation rate (see text)

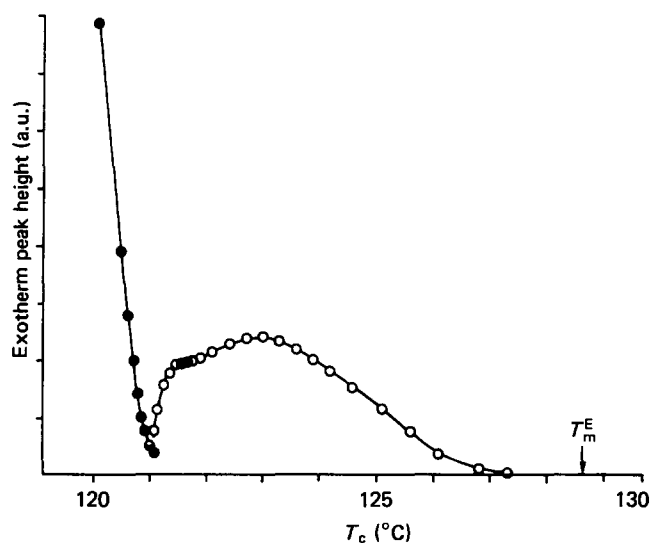


Figure 5 Maximum heat outflow,  $h_{\max}$ , during isothermal crystallization of  $C_{246}$  as a function of  $T_c$ . This parameter depends on the rate of crystal growth as well as on that of primary nucleation.  $\circ$ , chain-extended;  $\bullet$ , chain-folded crystallization

At this stage only the 'cleaner' parameter  $1/t_{10}$  could be analysed to any quantitative extent. As seen in Figure 4, at small supercoolings the primary nucleation rate starts to increase approximately exponentially with  $\Delta T$ . The downward departure from the exponential curve, i.e. the slow-down effect, starts above 125°C, 4°C above  $T^*$  and still well above the melting temperature of the chain-folded form. At its minimum, at 121.2°C, the primary nucleation rate is seen to be more than an order of magnitude lower than the value obtained for that temperature by extrapolating the initial exponential increase in  $1/t_{10}$ .

Parallel isothermal crystallization experiments were carried out at selected temperatures using synchrotron X-ray scattering. Figure 6 shows the development of the SAXS pattern of the E form (three diffraction orders) at 122.3°C. This temperature is slightly above  $T^*$ , where crystallization is greatly retarded already. No diffraction peaks other than those of the E form are present at any time. This behaviour contrasts with that at a somewhat lower temperature of 121.1°C (Figure 7), the temperature of the actual minimum in the crystallization rate (Figures 4 and 5). Here crystallization of NIF starts first. At some stage the chain-folded crystal lamellae, such as those already formed, thicken to the chain-extended form (at

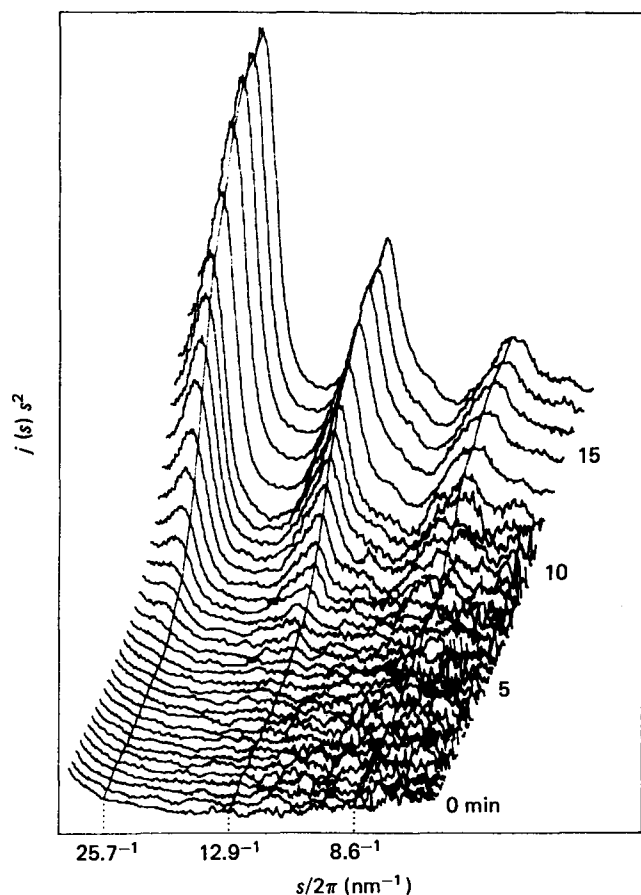


Figure 6 Series of consecutive SAXS curves (Lorentz corrected) recorded during unseeded melt-crystallization of  $C_{246}$  at  $T = 122.3^\circ\text{C}$ . Only extended-chain crystals appear, with chains tilted at  $35^\circ$  (three diffraction orders are visible). The three reference lines connect the ordinates at  $s/2\pi = 25.7^{-1}$ ,  $12.9^{-1}$  and  $8.6^{-1} \text{ nm}^{-1}$ , the inverse values of  $(L \cos 35^\circ)/n$ , where  $n = 1, 2, 3$  and  $L$  is the calculated extended-chain length (31.5 nm). Time in minutes is shown on the right. (Collection time: 12 s for each curve with 12 s pause. Last five curves: 60 s collection time)

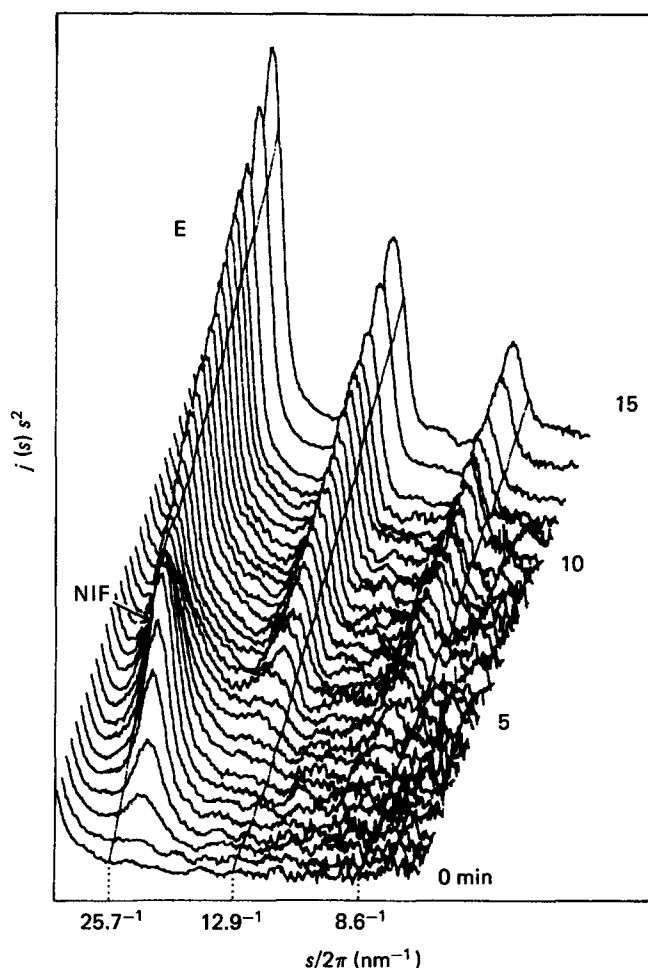


Figure 7 Series of consecutive SAXS curves (Lorentz corrected) recorded during unseeded melt-crystallization of  $C_{246}$  at  $121.1^\circ\text{C}$ . Folded-chain crystals (NIF) appear first; these subsequently transform into extended-chain crystals (E) with chains tilted at  $31^\circ$ . From  $t = 6$  min onwards only extended-chain crystallization is observed

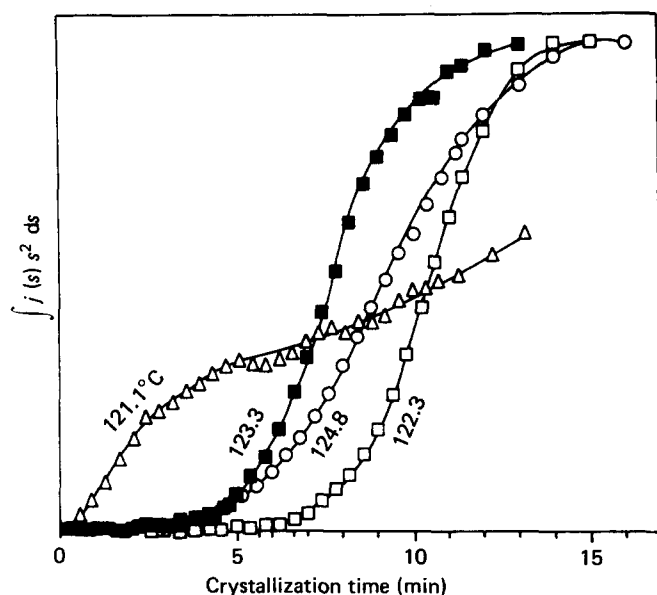


Figure 8 Time dependence of SAXS intensities integrated in the interval  $50^{-1} \text{ nm}^{-1} < s/2\pi < 7^{-1} \text{ nm}^{-1}$  during isothermal crystallization of  $\text{C}_{246}$ . Crystallization at  $121.1^\circ\text{C}$  is not followed to completion

around  $t = 4$  min). From there onwards only direct chain-extended crystallization takes place, as far as can be assessed from the absence of any reflections which are not due to the E form.

A fairly accurate measure of the progress of crystallization with time has been obtained from SAXS curves by integrating the background-subtracted and Lorentz-corrected diffraction intensities in the range 7–50 nm (Figure 8). Intensities integrated over this wide range give a reasonable approximation of the SAXS invariant. The crystallization curves at  $125.1^\circ\text{C}$ ,  $123.3^\circ\text{C}$  and  $122.3^\circ\text{C}$  have the characteristic sigmoidal shape. However, the  $121.1^\circ\text{C}$  curve is different: the 'induction period' is much shorter than that at higher temperatures. This clearly shows that folded-chain crystals take less time to nucleate than extended-chain ones, even though the former are supercooled by only *ca.*  $1.5^\circ\text{C}$  and the latter by as much as  $7.5^\circ\text{C}$  (see also below).

Comparing the crystallization rates at equal temperatures, as registered both by d.s.c. and by SAXS, the SAXS-based values are found to be consistently lower by a factor of 1.8. The difference may be due to enhanced primary nucleation on the aluminium surfaces of the d.s.c. pan relative to that in the glass capillary.

#### Preliminary self-seeding experiments

A number of features concerning the shape of the d.s.c. exotherms, such as peak asymmetry, particularly at temperatures just above  $T^*$ , or the appearance of double exotherms around or just below  $T^*$  (see later), indicate that it is the rate of primary nucleation rather than the crystal growth rate which exhibits the most conspicuous anomaly around  $T^*$ . Therefore, a few preliminary experiments were carried out in an attempt to establish whether both the growth rate and the primary nucleation rate exhibit the anomaly. The method of self-seeding, common in polymer crystallization studies<sup>7</sup>, was therefore used.

Preliminary self-seeded crystallization experiments by

d.s.c. indicated that the crystal growth rate itself does indeed slow down, or at least levels off as  $T_c$  is lowered towards  $T^*$ . However, attempts to obtain a quantitative temperature dependence of the growth rate alone were unsuccessful, as these were too high compared to the time scale of thermal equilibration of the instrument.

The second set of experiments was performed using the synchrotron X-ray source. The paraffin was first crystallized in the E form, and then the temperature was slowly increased up to the melting point and the scattering pattern observed. When most of the material had melted, leaving exactly 4% of the 'seed' crystals unmolten, the temperature was rapidly lowered to  $T_c$  and the crystallization followed as before. Two crystallization temperatures were chosen:  $122.3^\circ\text{C}$  and  $123.3^\circ\text{C}$ . The integrated diffraction intensities are plotted against crystallization time in Figure 9, alongside the parallel results for unseeded crystallization. As expected, the diffraction intensity started to increase immediately when seeds were present. The fact that it took approximately the same time for 'seeded' crystallization to reach completion as it took for unseeded crystallization (see curves for  $T_c = 123.3^\circ\text{C}$ ) indicates that the number of seeds was insufficient to induce all crystallization, and also that their distribution was probably non-uniform in the first place; thus many of the crystals which grew at the later stages were not nucleated on the pre-existing seed crystals, but developed from new nuclei. Nevertheless, the increase in crystallinity in the early stage can be regarded as entirely due to the growth of seed crystals, when the contribution of primary nucleation itself is still negligible. Thus, comparing the initial slopes of the two seeded crystallization curves it is evident that the rate of extended-chain crystal growth does *not* increase when supercooling is increased from  $5.3^\circ\text{C}$  ( $T_c = 123.3^\circ\text{C}$ ) to  $6.3^\circ\text{C}$  ( $T_c = 122.3^\circ\text{C}$ ). In fact it would appear that if anything it decreases slightly. Hence these results show that the anomaly near  $T^*$  is not restricted to primary nucleation, but applies also to crystal growth itself.

#### Observations on other paraffins

The same effect of retarded crystallization has so far also been observed in the preliminary experiments with

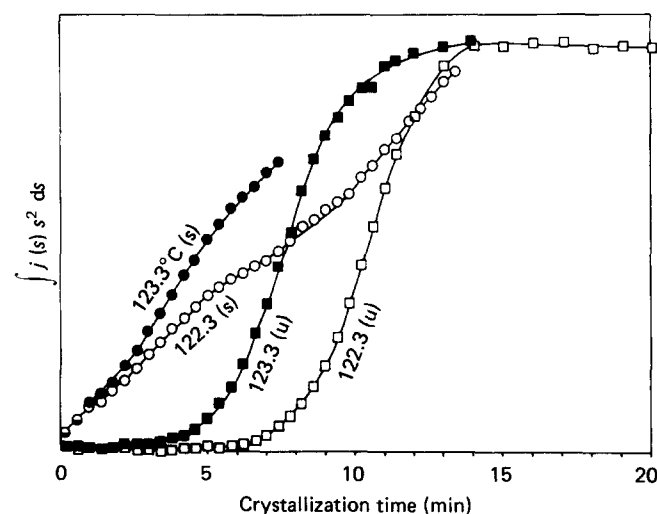


Figure 9 Integrated SAXS intensities for seeded (s) and unseeded (u) isothermal crystallization of  $\text{C}_{246}$ . Seeded crystallization runs were not followed to completion

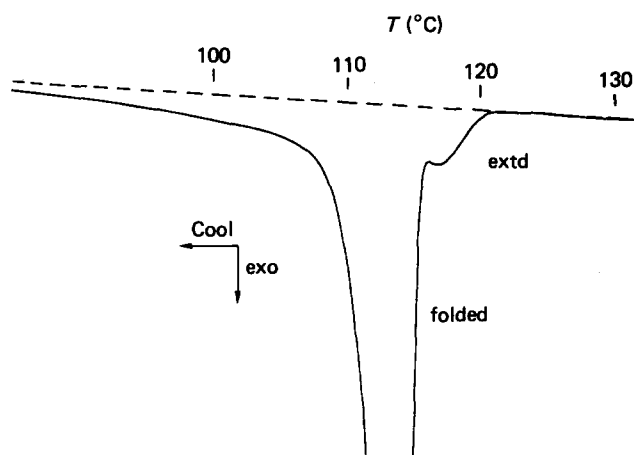


Figure 10 D.s.c. cooling scan of paraffin  $C_{198}$ ; cooling rate  $40^{\circ}\text{C min}^{-1}$

melt-crystallization of paraffin  $C_{198}H_{298}$  (see Figure 10), as well as in solution-crystallization studies of that alkane<sup>8</sup>. Figure 10 shows the crystallization thermogram of  $C_{198}$  during cooling at a constant rate of  $40^{\circ}\text{C min}^{-1}$ . Qualitative features are the same as those for  $C_{246}$  at the  $1^{\circ}\text{C min}^{-1}$  cooling rate (Figure 1). The reduction in crystallization rate (the dip between the extended- and folded-chain crystallization peaks) is more pronounced in the  $C_{198}H_{298}$  case.

Figure 10 provides the clearest and most unambiguous evidence that not only primary nucleation but also crystal growth slows down as  $T^*$  is approached from above. Then, if one bears in mind that only a small fraction of the melt has crystallized at the stage where the dip occurs (i.e. there can be no appreciable effect due to impingement of the growing crystals), the distinct minimum between the extended-chain and folded-chain exotherms cannot be interpreted in any other way but by a retardation in crystal growth. This is because in that case, even if primary nucleation ceased completely, the accelerated growth of the already existing crystals would result in a continuing increase in the overall measured crystallization rate as  $T_c$  was lowered.

## DISCUSSION

To our knowledge a reduction in crystallization rate with increasing supercooling of the kind observed here has not been reported previously for any polymeric system or for any crystallizable system in general. A decrease in crystallization rate at significantly larger supercoolings, arising from decreased mobility, i.e. higher viscosity of the liquid, is of course common, but is irrelevant to the present case; the glass transition temperature of polyethylene is more than  $200^{\circ}\text{C}$  below the temperature region of current concern.

In the  $\Delta T$  region, where the growth rate increases with  $\Delta T$ , this growth rate increase may display discontinuities observable in the case of sufficiently short and uniform chains such as reported first by Kovacs and coworkers in their salient studies on polyethylene oxides (see review<sup>9</sup>) and subsequently by Leung *et al.*<sup>10</sup> on polyethylene. The discontinuities correspond to changes from extended to once-folded, from once- to twice-folded etc. crystallization. Nevertheless, there the growth rate still increases all through with  $\Delta T$ . The actual decrease of crystallization

rate with increasing  $\Delta T$  well above temperatures where the transport term dominates is an altogether different phenomenon and cannot be rationalized along previously adopted lines.

In what follows we shall first discuss some of the experiments reported above in more detail. Then a qualitative explanation for the main effect, the retarded extended-chain crystallization near  $T^*$ , will be proposed.

### Qualitative analysis of experimental crystallization curves

**Retarded crystallization.** Inspection of the d.s.c. crystallization curves in Figure 3 and, in particular, the temperature dependence of the  $1/t_{10}$  parameter (Figure 4) leaves no doubt that the primary nucleation rate of paraffin  $C_{246}$  slows down with increasing supercooling, and that the slow-down begins well above  $T^*$ , the temperature at which chain-folded crystallization sets in. However, in addition it is worth restating here that the anomalous retardation is not limited to primary nucleation but extends also to crystal growth itself. The most direct evidence for this assertion comes from the cooling thermogram of  $C_{198}$ , and the assertion is further demonstrated by the SAXS results on the self-seeded crystallization of  $C_{246}$ , reported in the preceding section.

A further comment on the last experiment is in place here. The growth rate of pre-existing crystals at  $T_c = 122.3^{\circ}\text{C}$  (Figure 9) is only slightly lower than at  $123.3^{\circ}\text{C}$ ; at the same time unseeded crystallization at  $122.3^{\circ}\text{C}$  is much more retarded than at  $123.3^{\circ}\text{C}$ . Even though the retardation of growth is not as drastic as for primary nucleation, the mere fact that the growth rate at  $6.3^{\circ}\text{C}$  supercooling ( $T_c = 122.3^{\circ}\text{C}$ ) is not higher than at  $5.3^{\circ}\text{C}$  supercooling ( $T_c = 123.3^{\circ}\text{C}$ ) is in itself an anomaly. The increase in growth rate with  $\Delta T$  should be predictable from the kinetic theory of crystallization. Nevertheless, there is considerable latitude according to which variant of the theories is adopted. For the  $\Delta T$  interval in question the increase in rate ranges from as little as 20% to as much as 400%, depending on whether a linear or an exponential dependence pertains, respectively, which in turn depends on the choice of the parameter which identifies the apportioning of the free energy barrier between the attachment and detachment steps as laid out in the Appendix.

Accordingly, our main conclusion is that both primary nucleation and growth rates of extended-chain crystals show anomalous retardation, resulting in an inverted  $\Delta T$  dependence, as the transition temperature  $T^*$  between extended- and folded-chain crystallization is approached from above.

The exotherms in Figure 3 give information on the progress of overall crystallization. Certain conclusions about the temperature dependence of the rate of nucleation *versus* that of growth could be reached by their qualitative comparison. At low supercoolings the crystallization exotherms are fairly symmetrical and remain so down to  $T_c = 123^{\circ}\text{C}$ . It appears that the temperature coefficients of the primary nucleation rate and that of the growth rate are not too different in this temperature region.

The exotherms at  $121.7^{\circ}\text{C}$  and below are, in contrast, highly asymmetric. The initial crystallization period ( $t < t_{\text{max}}$ , where  $t_{\text{max}}$  is the time at which maximum heat evolution occurs) is greatly extended, and it is here that the nucleation rate anomaly is most prominent. The

$t > t_{\max}$  side of the exotherm is not extended proportionately. Thus we conclude next that the retardation in primary nucleation is greater than that in crystal growth.

**Double exotherms.** Within a narrow temperature range at and below  $T_c = 121.1^\circ\text{C}$  (Figure 3) the crystallization curves are characterized by double exotherms. Parallel SAXS experiments (Figure 7) show that the first exotherm (indicated with an asterisk in Figure 3) is due to the formation of once-folded chain crystals (NIF form) and the second exotherm emerging at longer times is due to the formation of extended-chain crystals. Figure 7 also shows that the initially grown chain-folded crystals thicken to the extended-chain form soon after their formation, and before or simultaneously with the appearance of the second exotherm.

The emergence of a second discrete exothermic peak during isothermal crystallization can, in principle, arise for two reasons. First, perfection of the as-formed crystals by reducing the non-crystalline fraction in the interlayers (known in polymers as 'secondary crystallization') takes place subsequent to the primary crystal formation. Secondly, the overall crystallization rate, which has already passed the maximum and is on its way down due to crystal impingement, experiences a net upturn as a consequence of an increase in the growth rate of individual crystals; thus the normal Avrami-type crystallization course is finished off at an accelerated rate. 'Secondary crystallization' indeed occurs in our crystallization runs below  $T^*$  to the extent that the as-formed F crystals isothermally thicken to produce E crystals. This is expected to result in some increase in crystallinity, but the resulting heat evolved cannot be nearly as high as ca. 50% of the total heat of crystallization necessary to explain the thermogram at  $121.0^\circ\text{C}$  (Figure 3); even less can 'secondary crystallization' account for the second exotherm containing ca. 80% of the total heat at  $121.1^\circ\text{C}$ . Moreover, if the second crystallization stage consisted mainly of a decrease in the ratio between the amorphous and crystalline layer thicknesses, the integrated SAXS intensity (the 'invariant') would pass through a maximum in the course of isothermal crystallization, with the intensity decreasing during the 'secondary crystallization' stage. On the contrary, the experiments show monotonously increasing intensities at all crystallization temperatures (Figure 8).

We are therefore left with the second interpretation, that the primary crystal growth rate steps up in the course of crystallization. The only feasible reason for this is a switch from folded- to extended-chain crystal growth triggered by the observed isothermal F  $\rightarrow$  E transformation of the already existing substrate crystals (Figure 7). It ought to be realized that both chain-extended and chain-folded growth can proceed on an E substrate, whichever is faster, whereas only chain-folded growth could take place on an F substrate that existed before the transformation. Thus the switch in crystal growth mode is clearly from folded- to extended-chain, implying therefore that the latter is faster. Thus we arrive at the important conclusion that, in a limited temperature range below the F melting point  $T_m^F$ , primary nucleation is faster for folded-chain crystals but growth is faster for extended-chain crystals.

Recognizing that there is a temperature range in which extended chains are favoured by crystal growth, and folded chains by primary nucleation, may in itself have important implications. The kinetic theory in its present form would not accommodate such a situation and, in fact, predicts the opposite trend: the critical fold length  $l^*$  of a primary nucleus is predicted to be always larger than that of the growth-determining secondary surface nucleus. In the case of homogeneous nucleation the ratio is 2:1 (for a review see ref. 11). (For more explicit details see ref. 6.)

#### The origin of retarded crystallization

We now arrive at the central question raised by the present experiments: why does crystallization, i.e. both nucleation and growth, of extended-chain paraffins slow down with increasing supercooling as the transition temperature  $T^*$  between extended- and folded-chain crystallization is approached? All current crystallization theories predict an increased rate with increasing supercooling provided the temperatures are well above that of the glass transition (see Appendix).

Let us consider the free energy of crystallization  $\Delta F$  as a function of the fold period  $l$ . As opposed to the continuous  $\Delta F(l)$  dependence in polydisperse polymers, for a uniform long alkane,  $\Delta F(l)$  can be approximated by a step function, as schematically drawn in Figure 11. The stepwise increase in  $\Delta F$  occurs at each point where  $l$  is reduced below a given  $L/n$  value, where  $L$  is the extended chain length and  $n$  an integer. At each such point the number of folds per molecule is increased from  $n-1$  to  $n$ , resulting in a corresponding increase in internal energy. (Recent statistical thermodynamic analysis of the  $\Delta F(l)$  function<sup>6</sup> shows that  $\Delta F$  is not constant between the individual steps, as drawn in Figure 11, but has a more complex shape with a minimum and a maximum within a given interval  $L/(n+1) < l < L/n$ . The simplified step function in Figure 11, however, should suffice for the

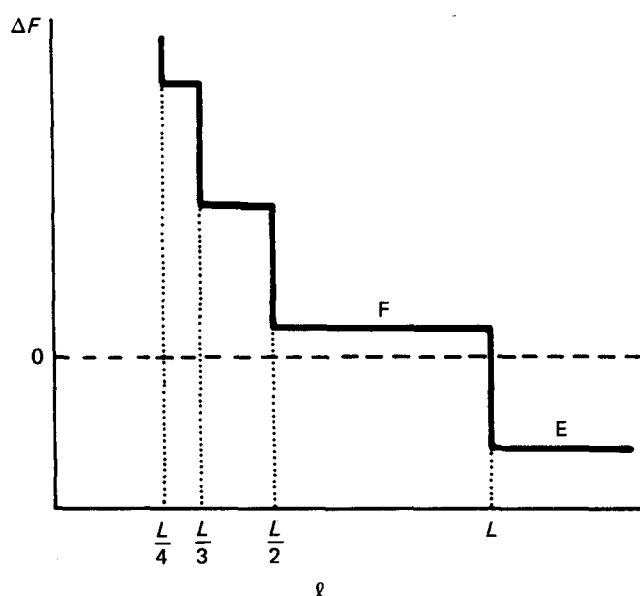


Figure 11 Free energy of crystallization of a uniform long paraffin as a function of fold length (schematic).  $L$  is the extended chain length. The situation with the  $\Delta F = 0$  line as drawn corresponds to a temperature slightly above  $T_m^F$ .

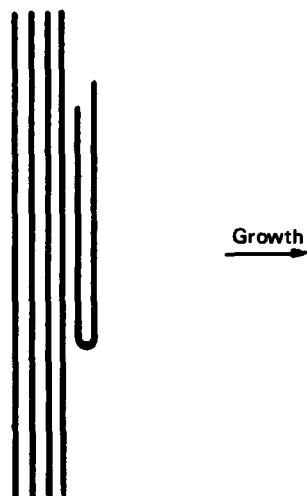


Figure 12 A possible instantaneous arrangement of molecules on the surface of a growing crystal at a temperature slightly above  $T_m^F$

present considerations. In particular,  $\Delta F$  appears to be fairly flat in the region of  $l$ s that were actually observed for the once-folded structure, i.e. in the lower part of the  $L/2 \leq l < L$  interval. This is deduced from the close proximity of the F2 and NIF melting points  $T_m^{F2}$  and  $T_m^{NIF}$ . Thus, for the purpose of the present discussion, we neglect the difference between NIF and F2 and refer to these forms collectively as the folded structure (F)).

As the temperature is lowered through the melting points of the different folded forms the zero level ( $\Delta F = 0$ ) in Figure 11 (broken horizontal line) moves upward. In the temperature interval  $T_m^F < T < T_m^E$ , only extended chain nuclei can lead to growth of stable crystals with  $\Delta F < 0$ . According to the kinetic theory the change in crystallization rate in this temperature interval should be determined exclusively by the driving force  $\Delta F$ , since the surface free energy barrier for deposition of new stems is constant as  $l$  is constant. Thus the rate would monotonously increase with  $\Delta T$  (see Appendix).

However, as  $T_m^F$  is being approached from above another process appears to interfere with extended-chain crystallization, decreasing its rate. This retardation of crystallization in the E form starts well above  $T_m^F$ , and becomes increasingly significant as  $T_m^F$  is approached. One would expect this retarding factor to be due to the onset of chain folding, even though folded structures cannot as yet be stable at these temperatures.

Taking the case of crystal growth first, it would appear that the interference is caused by temporarily attached folded molecules reducing the growth surface available for productive extended chain deposition (see Figure 12). Although at  $T > T_m^F$  the average lifetime of each individual folded configuration is bound to be very short, except for temperatures extremely close to  $T_m^F$ , it is the large number of possible folded molecular conformations, multiplied by the number of possible positions along the potential extended-chain sites, that makes the high partial coverage of these sites by folded molecules a viable possibility. Due to the increasing lifetime of folded depositions the surface obstruction would inevitably become enhanced, approximately exponentially, as the temperature is decreased towards  $T_m^F$ .

A similar retardation mechanism is also envisaged to operate for primary nucleation. In this case, however, it

can be assumed that no extended chains are present in a primary subcritical nucleus for a considerable time. The probability of the chains extending fully, relative to their folding back on themselves, is even lower in primary nucleation where as yet there is no substrate along which to extend. It may be said that, although only extended-chain nuclei can eventually lead to productive growth above  $T_m^F$ , this is not 'obvious' to the depositing chains at the outset; they will be mostly 'misled' into participating in unproductive chain-folded fluctuations which evidently involve a significantly lower free-energy barrier than do extended-chain ones.

## CONCLUSION

To our knowledge a minimum in the crystallization rate (including both primary nucleation and growth) with supercooling is unprecedented not only for polymers, but for crystallization in general. It is apparent that this is the result of competition between crystallization in different chain configurations, which in the case examined here are the fully extended (E) and once-folded (NIF)<sup>5</sup> forms. The existence of this phenomenon, and the way it occurs, seem to be a unique manifestation of polymer crystallization involving chain folding, with substantial new and subtle information content regarding the nature of the crystallization process, of potential importance for its understanding. This is one of the several, hitherto hidden, features of polymer crystallization which has become accessible through the availability of strictly uniform long-chain n-alkanes.

## ACKNOWLEDGEMENTS

We are greatly indebted to Professor M. C. Whiting and Dr I. Bidd (Organic Chemistry, Bristol) for the synthesis of the long n-alkanes. We wish to thank Professor Whiting in particular for handing over unique material and for numerous helpful discussions. G. Ungar wishes to thank the Science and Engineering Research Council for financial support.

## REFERENCES

- Paynter, D. I., Simmonds, D. J. and Whiting, M. C. *J. Chem. Soc., Chem. Commun.* 1982, 1165
- Bidd, I. and Whiting, M. C. *J. Chem. Soc., Chem. Commun.* 1985, 543
- Ungar, G., Stejny, J., Keller, A., Bidd, I. and Whiting, M. C. *Science* 1985, **229**, 386
- Organ, S. and Keller, A. *J. Polym. Sci.* in press
- Ungar, G. and Keller, A. *Polymer* 1986, **27**, 1835
- Ungar, G. in 'Integration of Fundamental Polymer Science and Technology' (Eds P. J. Lemstra and L. Kleintjens), Vol. 2, Elsevier—Applied Science, London, in press
- Blundell, D. J. and Keller, A. *J. Macromol. Sci.* 1968, **B2**, 301
- Organ, S., Keller, A. and Ungar, G. in preparation
- Buckley, C. P. and Kovacs, A. J. in 'Structure of Crystalline Polymers', (Ed. I. H. Hall), Elsevier—Applied Science, London, 1984, p. 261
- Leung, W. M., Manley, R. J. and Panaras, A. R. *Macromolecules* 1985, **18**, 760
- Wunderlich, B. 'Macromolecular Physics', Academic Press, New York, 1976, Vol. 2
- Hoffman, J. D. *Macromolecules* 1985, **18**, 772
- Frank, F. C. and Tosi, M. *Proc. R. Soc. Lond.* 1961, **263**, 323
- Hoffman, J. D., Davis, G. T. and Lauritzen, J. I. Jr. in 'Treatise in Solid State Chemistry', (Ed. N. B. Hannay), Plenum Press, New York, 1976, p. 497
- Sadler, D. M. *J. Polym. Sci., Polym. Phys. Edn.* 1985, **23**, 1533



## APPENDIX

For the specific case of extended-chain crystallization of monodisperse flexible chains Hoffman<sup>12</sup> derives the following expression for the growth rate:

$$G = N_0 b \beta \exp\left[-(2bl\sigma + 2ab\sigma_e)/kT\right] \{1 - \exp[-(abl\Delta h_f/T_m kT)(T_0 - T)]\} \quad (1)$$

Here  $N_0$  is the number of reacting species,  $\beta$  is a transport term,  $a$  and  $b$  are lateral chain dimensions,  $\sigma$  and  $\sigma_e$  the side and end surface free energies,  $\Delta h_f$  the heat of fusion, and  $T_0$  the highest temperature for finite rate growth ( $T_0$  is very close to  $T_m$  for extended chains). For small supercoolings the last exponential term can be expanded in series, showing the crystallization rate to be a nearly linearly increasing function of effective supercooling:

$$G \propto T_0 - T \quad (2)$$

We note, however, that on the basis of earlier versions of the nucleation theory of polymer crystallization one would predict an exponential increase in growth rate on supercooling. Thus, from the expression for secondary nucleation rate given by Frank and Tosi<sup>13</sup>, the ratio of growth rates at two different relatively small supercoolings  $\Delta T_1$  and  $\Delta T_2$  is derived as:

$$\frac{G_1}{G_2} = \left[ \frac{\exp(A\Delta T_1)}{\exp(A\Delta T_2)} \right] \left[ \frac{1 - \exp(B - A\Delta T_1)}{1 - \exp(B - A\Delta T_2)} \right] \quad (3)$$

with  $A$  and  $B$  being practically constant for fixed  $l$ :

$$A = \frac{abl\Delta h_f}{kT_m} \quad B = \frac{2ab\sigma_e}{kT}$$

Expanding the numerator and denominator of the second fraction on the right-hand side of (3), we obtain:

$$G_1/G_2 = (\Delta T_1/\Delta T_2) \exp(\Delta T_1 - \Delta T_2)$$

Here the exponential term is dominant and the ratio of our two growth rates at 6.3°C and 5.3°C supercoolings (see Discussion) would accordingly be 5:1. In contrast, by the linear relationship (2) this ratio would only be 1:1.2. The fundamental difference between the two approaches leading to such different growth rate dependences on  $\Delta T$  is in the way the activated state in stem deposition is defined. While the first<sup>12</sup> assumes that the activated transition state has its free-energy raised by the creation of new surface, but without it simultaneously being reduced to any extent by the release of bulk free energy of crystallization ('parameter  $\psi$ '<sup>14</sup> = 0), the second (earlier version) assumed full release of the bulk free energy simultaneously with the creation of new surface ( $\psi = 1$ ). It may be argued that the two approaches represent two extremes, an intermediate situation probably being more realistic.

We note that the alternative crystallization theory of polymers, i.e. the 'rough-surface growth' theory predicts a linear  $\Delta T$  dependence of the crystal growth rate within a given 'branch' (extended, once-folded etc.) for uniform chain systems<sup>15</sup>.

**Note added in proof**

Current rate equation treatment of 'rough surface' crystal growth is showing that minima similar to those observed here can indeed be expected if the free energy of crystallization has discrete minima at specific values of crystal thickness (Sadler, D. M. and Gilmer, G. H. *Polym. Commun.* 1987, **28**, 242).